The three EPR g values (g_3 = 2.234, g_2 = 2.074, g_1 = 2.050), in agreement with the geometry of the complex, are very similar to those reported for other elongated octahedral complexes[5,12a,20] with the CuN_2O_4 chromophore.

The room-temperature electronic spectrum of our compound, which shows a broad maximum centered at 15.9×10^3 cm^{-1} (Table IV), also indicates an elongated octahedral ligand field with a CuN_2O_4 chromophore.

In Table IV the Cu···O axial distances, the distortion angles, and the electronic spectra for a series of similar complexes are compared. It is observed that for complexes **2**, **3**, **5**, and **6**, which show axial and equatorial copper–ligand bond lengths comparable, there is a dependence of the electronic spectra on the distortion angles. In fact this angle is a measure of the metal–ligand orbital overlap, which increases as the angle decreases.[21] Therefore, for complexes **1**, **2**, and **3**, the Cu–O axial contact must be considered a true bond interaction, and their d–d band maximum is consistent with an elongated tetragonal-octahedral stereochemistry.[5] For complexes **5** and **6**, the value of the angle indicates an effective square-planar geometry as suggested from the d–d spectra.[21] All this reinforces the utility of electronic absorption spectroscopy in elucidating the probable coordination geometry of a metal ion.

The more relevant bands of the IR spectrum of the present complex are reported in Table V and compared with those of the other structurally known copper(II)–*N*-tosylglycinate complexes.[2,3] The main differences between deprotonated (complexes **7** and **8**) and undeprotonated (complexes **9** and **10**) in *N*-tosylglycinate derivatives are observed in the NH, SO_2, and SN stretching frequency regions. In fact, $\nu(SO_2)$ and $\nu(SN)$ at lower and higher energies, respectively, in complexes **7** and **8** than in complexes **9** and **10** is a consequence of the lengthening of the S–O bond and the shortening of the S–N bond due to the sulfonamide nitrogen deprotonation (ν(NH) is absent in deprotonated complexes). In complexes **9** and **10** ν(NH) appears at greater energy in the 4-methylpyridine adduct than in the *N*-methylimidazole adduct as, in the first complex, the NH group is involved only in one hydrogen-bonding interaction. It is also worthy of note that for all the complexes reported in Table V there are no appreciable differences in band shapes and positions of the carboxylate stretching frequencies even though they are differently involved in the copper coordination. The presence of hydrogen bonding in which these groups are also involved makes this technique insufficient for assigning the coordination type of the carboxylate group.

As regards the pyridine adduct, we did not obtain suitable crystals for X-ray analysis but the strict similarity of the physical properties (μ_{eff} = 1.83 μ_B; $g_\parallel$ = 2.242, $g_\perp$ = 2.076) and, in particular, of the d–d band shape and position (15.6×10^3 cm^{-1}), with those of the 4-Mepy adduct enables us tentatively to suggest the presence of an octahedral copper(II) environment also in this complex.

Acknowledgments. The authors thank the Centro Strumenti of the University of Modena for IR recording and Prof. G. C. Pellacani for the helpful discussion.

Registry No. [Cu(TsglyH)$_2$(4-Mepy)$_2$·H_2O], 86365-39-1; [Cu(TsglyH)$_2$(py)$_2$·H_2O], 86365-41-5; [Cu(TsglyH)$_2$·$4H_2O$], 86391-46-0.

Supplementary Material Available: Listings of van der Waals contacts, thermal parameters and bond distances for hydrogen atoms, anisotropic thermal parameters, selected least-squares planes, and final structure factors (17 pages). Ordering information is given on any current masthead page.

(19) The lack of an apparatus that can achieve temperatures near 0 K, as required for an unambiguous explanation of magnetic properties of similar monobridged copper(II) complexes, prevented us from verifying this hypothesis.
(20) Yokoi, H.; Sai, M.; Isobe, T.; Oshawa, S. *Bull. Chem. Soc. Jpn.* **1972**, *45*, 2189.
(21) Hathaway, B. J.; Billing, D. E. *Coord. Chem. Rev.* **1970**, *5*, 143.

Contribution from the Department of Chemistry, University of Delaware, Newark, Delaware 19711

Synthesis, Crystal Structure, and Molecular Geometry of $[(\eta^5\text{-}C_5H_5)_2Fe]_4[Bi_4Br_{16}]$, the Ferrocenium Salt of a "Cluster of Octahedra" Hexadecabromotetrabismuthate Counterion

ARNOLD L. RHEINGOLD,* ALLEN D. UHLER,[1] and ALBERT G. LANDERS[2]

Received February 13, 1983

Ferrocene in the presence of sunlight, $BiBr_3$, and molecular oxygen is oxidized to the ferrocenium cation and precipitates as the crystalline product $[(\eta^5\text{-}C_5H_5)_2Fe]_4[Bi_4Br_{16}]$ along with a stoichiometric quantity of BiOBr. The ferrocenium salt crystallizes in the monoclinic space group $P2_1/c$ with a = 14.294 (4) Å, b = 19.337 (3) Å, c = 12.269 (2) Å, β = 109.23 (2)°, V = 3202.1 (13) Å^3, and Z = 2. The asymmetric unit consists of one-half anion and two independent cations. The structure was refined to discrepancy indices of R_F = 5.5% and R_{wF} = 5.5% for those 3202 reflections with $I > 3\sigma(I)$. The $(\eta^5\text{-}C_5H_5)_2Fe^+$ cations are unusual in that the inter-ring alignments are neither symmetrically staggered nor eclipsed; rather the angles of displacement are 7.3 and 23.4° from an eclipsed configuration. The $Bi_4Br_{16}^{4-}$ anion is the first example of a cluster of four edge-sharing distorted $BiBr_6$ octahedra. The terminal Bi–Br bond distances average 2.683 Å while the bridging Bi–Br bond distances average 3.025 Å. The structure is compared to other crystallographically characterized polybromobismuthate anions. A review of these data reveals a trans effect in bond distances as previously predicted from a force constant analysis of vibrational data.

Introduction

We previously reported the synthesis and crystallographically determined structures of the ferrocenium ion $(\eta^5\text{-}C_5H_5)_2Fe^+$ salts formed by the photochemically promoted oxidation of ferrocene by molecular oxygen in the presence of the group 5 trichlorides $AsCl_3$,[3] $SbCl_3$,[4] and $BiCl_3$.[5] In each

(1) Current address: Department of Chemistry, University of Maryland, College Park, MD.
(2) Current address: Armstrong World, Lancaster, PA.
(3) Churchill, M. R.; Landers, A. G.; Rheingold, A. L. *Inorg. Chem.* **1981**, *20*, 849.
(4) Rheingold, A. L.; Landers, A. G.; Dahlstrom, P. L.; Zubieta, J. *J. Chem. Soc., Chem. Commun.* **1979**, 143.

0020-1669/83/1322-3255$01.50/0

case the anion was complex and for the As- and Sb-based salts contained oxygen, specifically $As_4Cl_{10}O_2^{2-}$ (two $Cl_2AsOAsCl_2$ moieties are joined by triply bridging Cl^- ions), $Sb_8Cl_{24}O_2^{4-}$ (four $SbCl_3$ and two $Cl_2SbOSbCl_2$ moieties are joined by doubly bridging and quadruply bridging Cl^- ions), and $BiCl_4^-$ (infinite chain of edge-sharing $BiCl_6^{3-}$ octahedra). Stoichiometrically compatible quantities of EOCl (E = As, Sb, or Bi) accompany the formation of the $(\eta^5\text{-}C_5H_5)_2Fe^+$ salts.

We have suggested[4] that these reactions proceed via the electrophilic attack of ECl_2^+ at Fe to produce the ferrocenonium ion $(\eta^5\text{-}C_5H_5)_2FeECl_2^+$, which is photochemically activated to oxidation by molecular oxygen, i.e.

$$2ECl_3 \rightleftharpoons ECl_2^+ + ECl_4^-$$

$$ECl_2^+ + (\eta^5\text{-}C_5H_5Fe)_2 \rightarrow (\eta^5\text{-}C_5H_5)_2FeECl_2^+$$

$$(\eta^5\text{-}C_5H_5)_2FeECl_2^+ \xrightarrow[O_2]{h\nu} (\eta^5\text{-}C_5H_5)_2Fe^+ + EOCl + \text{various complex anions}$$

E = As, Sb, or Bi

Supporting these mechanistic assertions are the following observations: (1) conductivity studies of $AsCl_3$, $SbCl_3$, and $BiCl_3$ in acetonitrile support an autoionization process;[6] (2) unsubstituted ferrocene is photochemically (vis–UV) inert in oxygen-saturated solvents such as hydrocarbons, acetone, and acetonitrile and other solvents in which the electronic spectrum of ferrocene does not display significant solvent effects;[7] (3) electrophilic attack at Fe has been observed in other metallocene–metal halide systems, and irradiation of subsequently formed adducts leads to metallocenium ion formation;[8] and (4) no product formation occurs in thoroughly degassed solvents.

The overall reaction may be represented as

$$4(\eta^5\text{-}C_5H_5)_2Fe + 6BiBr_3 + O_2 \rightarrow [(\eta^5\text{-}C_5H_5)_2Fe]_4[Bi_4Br_{16}] + 2BiOBr$$

A study using chlorine and bromine NQR spectroscopy revealed that the salts $(\eta^5\text{-}C_5H_5)_2FeBiCl_4$ and $(\eta^5\text{-}C_5H_5)_2FeBiBr_4$ possessed quite different structures.[9] At the time of this study, the structure of the chloride salt was known but that of the bromide was not. We have now characterized the bromide salt by X-ray diffraction techniques and find that, unlike the infinite-chain structure of the chloride salt, the bromide salt is formulated $[(\eta^5\text{-}C_5H_5)_2Fe]_4[Bi_4Br_{16}]$, with the anion adopting a novel structure describable as a cluster of four distorted edge-sharing $BiBr_6$ octahedra.

The range of structural types of crystallographically characterized polybromobismuthate ions is remarkable (see Table III) and suggests that, from the many anion structures possible, the one found in the solid state accompanying a particular cation may be largely determined by a maximization of lattice energy.[10] Similar effects have also been noted in polybromoantimonate ions.[11]

The 2-picolinium ion salt [2-picolinium][$BiBr_4$] has the same empirical anion formula as the title compound but crystallizes with the infinite-chain, edge-sharing octahedra anion structure.[12]

Experimental Section

A. Preparation of $[(\eta^5\text{-}C_5H_5)_2Fe]_4[Bi_4Br_{16}]$. To 100 mL of Spectrograde acetone containing 0.62 g (3.3 mmol) of ferrocene was added 1.49 g (3.3 mmol) of freshly prepared $BiBr_3$ (obtained from Bi and Br_2 and recrystallized from $CHCl_3$). The resulting solution was swirled in a 250-mL flask for a few minutes to saturate with air, stoppered, and allowed to remain undisturbed in a sunny window. Within minutes of initial exposure, shiny blue-black crystals began to form, which were allowed to grow for 7 days to achieve a crystallographically useful size. A finely divided white sludge formed along with the blue-black crystals. After removal of most of the acetone by evaporation, the residue was suspended in 20 mL of diiodomethane. After the mixture was allowed to stand undisturbed for 24 h, a complete separation of the white and blue-black products was achieved by their relative densities. The blue-black crystals floated; the white sludge sank. A 21% yield (0.51 g) of $[(\eta^5\text{-}C_5H_5)_2Fe]_4[Bi_4Br_{16}]$, on the basis of ferrocene, was obtained as bladelike, well-formed blue-black crystals (thin sections appear wine red by transmitted light). The white material collected from the bottom of the flask (0.16 g) was identified as BiOBr by elemental analysis. The ferrocenium salt was insoluble in most organic solvents, slightly soluble in acetonitrile, and very soluble in water. Aqueous solutions rapidly decomposed, forming $(\eta^5\text{-}C_5H_5)FeFeBr_4$ and other unidentified products.

Anal. Calcd: C, 16.81; H, 1.41; Fe, 7.82; Bi, 29.24; Br, 44.73. Found: C, 16.16; H, 1.30; Fe, 7.66; Bi, 29.37; Br, 44.36.

In the absence of light, a blue-gray microcrystalline product was obtained in very low yield, which provided an elemental analysis similar to that of the product formed in sunlight. In well-degassed and -dried systems, no crystalline products were obtained after a 2-month exposure to sunlight.

B. Crystallography of $[(\eta^5\text{-}C_5H_5)_2Fe]_4Bi_4Br_{16}$. X-ray Data Collection. The data crystal (dimensions 0.03 × 0.12 × 0.43 mm) was obtained by cleavage from a larger flat needle crystal. Lattice parameters were obtained from the angular settings of 25 accurately centered reflections, $25° \leq 2\theta \leq 35°$. Intensities were collected for 4127 reflections by using a Nicolet R3 diffractometer and θ–2θ scan techniques ($\pm h, +k, +l$) at room temperature with $4° \leq 2\theta \leq 45°$ at a variable scan rate (3–10°/min). After equivalent reflections were merged (agreement error on averaged reflections 1.78%), there remained 3739 reflections, of which 3202 with $I > 3\sigma(I)$ were used for all calculations. An empirical correction for absorption was used (maximum transmission/minimum transmission = 0.147/0.113). Programs used are contained in the Nicolet SHELXTL, XTL, XP, and P3 program packages.

Structure Solution and Refinement. The structure was solved by the direct-methods routine SOLV ($E_{min} = 2.0$, $E_{ref} = 0.25$) and refined to minimum values of $\sum w\Delta^2$ ($\Delta = |F_o| - |F_c|$; $w^{-1} = \sigma^2(F_o) + 0.0015|F_o|^2$). The cyclopentadienyl rings were refined with hydrogen atom restraints to hold all C–H distances equal to 0.96 Å and isotropic thermal parameters equal to 1.2 times the value for the C atom to which it was attached. Anisotropic thermal parameters were employed for all non-hydrogen atoms. The final R ($=\sum|\Delta|/\sum|F_o|$) was 0.055. The asymmetric unit consists of two independent ferrocenium ions and half of a $Bi_4Br_{16}^{4-}$ anion, the center of which coincides with an inversion center.

The final difference map revealed numerous peaks in the vicinity of the Bi atoms in the range 1.0–1.5 e/Å^3, the result likely of an inadequate correction for absorption (μ = 220.3; plate-shaped specimen). No systematic trends as a function of indices, sin θ, or $|F_o|$ were observed.

Atomic coordinates, thermal parameters, complete listing of bond distances and angles, and a list of F_o vs. F_c values are available as supplementary data.

Results and Discussion

Final atomic positional parameters are provided in Table II, and selected interatomic distances and angles are given in

(5) Landers, A. G.; Lynch, M. W.; Raaberg, S. B.; Rheingold, A. L.; Lewis, J. E.; Mammano, N. J.; Zalkin, A. *J. Chem. Soc., Chem. Commun.* **1976**, *931*. Mammano, N. J.; Zalkin, A.; Landers, A.; Rheingold, A. L. *Inorg. Chem.* **1977**, *16*, 297.
(6) Rheingold, A. L.; Sheats, G. S., unpublished results.
(7) Tarr, A. M.; Wiles, D. M. *Can. J. Chem.* **1968**, *46*, 2725. Traverso, O.; Carassiti, V. *Gazz. Chim. Ital.* **1974**, *104*, 1033.
(8) Bitterwolf, T. E.; Ling, A. C. *J. Organomet. Chem.* **1972**, *40*, C29. Coyle, J. D.; Marr, G. *Ibid.* **1973**, *60*, 153. Bitterwolf, T. E.; Ling, A. C. *Ibid.* **1972**, *40*, 197. Morrison, W. H.; Hendrickson, D. N. *Inorg. Chem.* **1972**, *11*, 2912. Traverso, O.; Chiorboli, C.; Mazzi, U.; Zucchini, G. *Gazz. Chim. Ital.* **1977**, *107*, 181.
(9) Landers, A. G.; Brill, T. B. *Inorg. Chem.* **1980**, *19*, 744.
(10) Whealy, R. D.; Scott, J. C. *Inorg. Chim. Acta* **1967**, *1*, 479. Whealy, R. D.; Osborne, J. F. *Ibid.* **1970**, *4*, 420.
(11) Porter, S. K.; Jacobsen, R. A. *J. Chem. Soc. A* **1970**, 1359.
(12) Robertson, B. K.; McPherson, W. G.; Myers, E. A. *J. Phys. Chem.* **1967**, *71*, 3531.

Table I. Crystal and Refinement Data for $[(\eta^5\text{-}C_5H_5)_2Fe]_4[Bi_4Br_{16}]$

formula	$[(C_5H_5)_2Fe]_4Bi_4Br_{16}$
fw	2858.50
cryst syst	monoclinic
space group	$P2_1/c$
a, Å	14.294 (4)
b, Å	19.337 (3)
c, Å	12.269 (2)
β, deg	109.23 (2)
V, Å^3	3202.1 (13)
Z	2
ρ(obsd), ρ(calcd), g/cm^3	2.93, 2.96
temp, °C	23
cryst dimens, mm	0.03 × 0.12 × 0.43
radiation	graphite-monochromated Mo Kα (λ = 0.710 73 Å)
diffractometer	Nicolet R3
abs coeff, cm^{-1}	220.3
scan speed, deg/min	3–10 (variable)
2θ scan range, deg	$4 \leq 2\theta \leq 45$
scan technique	$\theta/2\theta$
data collcd	$\pm h, +k, +l$
ignorance factor, g[a]	0.0015
no. of unique data	3739 reflcns (4127 collcd)
no. of unique data with $(F_o)^2 > 3\sigma(F_o)^2$	3202
std reflcns	3/141 (no decay obsd)
R, %	5.5
R_w, %	5.5
GOF	1.241

[a] $w^{-1} = \sigma^2(F_o) + g|F_o|^2$.

Table II. Fractional Atomic Coordinates (×10^4) for $[(\eta^5\text{-}C_5H_5)_2Fe]_4[Bi_4Br_{16}]$

atom	x	y	z
Bi(1)	5501 (1)	6069 (1)	4728 (1)
Bi(2)	2169 (1)	5490 (1)	3526 (1)
Br(1)	4140 (1)	4946 (1)	3196 (2)
Br(2)	3726 (2)	6543 (1)	5049 (2)
Br(3)	7214 (2)	5450 (1)	4318 (2)
Br(4)	5339 (2)	6958 (1)	3018 (2)
Br(5)	6552 (2)	6936 (1)	6376 (2)
Br(6)	860 (2)	4506 (1)	2455 (2)
Br(7)	806 (2)	6280 (1)	3993 (2)
Br(8)	1977 (2)	6131 (1)	1514 (2)
Fe(1)	3083 (2)	8771 (1)	3576 (2)
Fe(2)	1476 (2)	1770 (1)	4699 (2)
C(11)	1611 (14)	8768 (11)	3418 (18)
C(12)	1654 (15)	8957 (12)	2382 (19)
C(13)	2146 (18)	8408 (14)	2000 (18)
C(14)	2348 (19)	7893 (13)	2848 (23)
C(15)	2019 (16)	8129 (13)	3737 (18)
C(16)	4148 (24)	9478 (17)	3483 (31)
C(17)	3837 (21)	9594 (14)	4464 (39)
C(18)	4095 (20)	9006 (18)	5081 (21)
C(19)	4555 (16)	8590 (13)	4563 (26)
C(20)	4507 (18)	8871 (15)	3607 (23)
C(21)	2266 (21)	1357 (10)	3706 (19)
C(22)	2829 (19)	1390 (13)	4856 (24)
C(23)	2437 (21)	997 (11)	5455 (21)
C(24)	1593 (21)	711 (11)	4749 (23)
C(25)	1452 (18)	939 (11)	3616 (22)
C(26)	1064 (23)	2793 (10)	4345 (25)
C(27)	1640 (19)	2715 (11)	5531 (27)
C(28)	1158 (17)	2275 (11)	6021 (21)
C(29)	293 (18)	2075 (13)	5150 (26)
C(30)	237 (18)	2414 (12)	4172 (21)

Table III. A view of the packing of $(\eta^5\text{-}C_5H_5)_2Fe^+$ and $Bi_4Br_{16}^{4-}$ ions in the unit cell is shown in Figure 1.

The Ferrocenium Ions. Two independent $(\eta^5\text{-}C_5H_5)_2Fe^+$ ions appear in the crystallographic asymmetric unit. The η^5-cyclopentadienyl ligands are each planar within the limits of experimental error. The Fe atoms lie symmetrically between the rings; Fe(1) is 1.694 (6) Å from the planes defined by atoms C(11)–C(15) and C(16)–C(20), and Fe(2) is 1.692 (7) Å from the C(21)–C(25) plane and 1.702 (6) Å from the C(26)–C(30) plane. The dihedral angle between these planes for Fe(1) is 2.0° and for Fe(2) is 6.4°. A point of particular interest is that, in contrast to all previously determined ferrocenium ion structures,[3-5,13-16] the η^5-C_5H_5 rings are not

Table III. Selected Bond Distances and Angles for $[(\eta^5\text{-}C_5H_5)_2Fe]_4[Bi_4Br_{16}]$ with Esd's

(a) Bond Distances (Å)

Bi(1)-Br(1)	3.101 (4)	Bi(2)-Br(1)	3.156 (4)
Bi(1)-Br(2)	2.844 (4)	Bi(2)-Br(2)	3.139 (4)
Bi(1)-Br(3)	2.914 (4)	Bi(2)-Br(6)	2.689 (4)
Bi(1)-Br(4)	2.663 (4)	Bi(2)-Br(7)	2.681 (4)
Bi(1)-Br(5)	2.689 (4)	Bi(2)-Br(8)	2.694 (4)
Bi(1)-Br(1′)	3.122 (4)	Bi(2)-Br(3′)	3.089 (4)
av Bi-Br(term)	2.683	av Bi-Br(bridg)	3.052
av Fe(1)-C	2.051	av Fe(2)-C	2.059

(b) Bond Angles (deg)

Br(1)-Bi(1)-Br(2)	84.2 (1)	Br(1)-Bi(2)-Br(7)	163.6 (1)
Br(1)-Bi(1)-Br(3)	90.2 (1)	Br(2)-Bi(2)-Br(7)	85.7 (1)
Br(2)-Bi(1)-Br(3)	174.1 (1)	Br(6)-Bi(2)-Br(7)	94.0 (1)
Br(1)-Bi(1)-Br(4)	95.8 (1)	Br(1)-Bi(2)-Br(8)	82.0 (1)
Br(2)-Bi(1)-Br(4)	92.9 (1)	Br(2)-Bi(2)-Br(8)	94.9 (1)
Br(3)-Bi(1)-Br(4)	89.4 (1)	Br(6)-Bi(2)-Br(8)	91.9 (1)
Br(1)-Bi(1)-Br(5)	168.7 (1)	Br(7)-Bi(2)-Br(8)	94.1 (1)
Br(2)-Bi(1)-Br(5)	89.9 (1)	Br(1)-Bi(2)-Br(3′)	84.2 (1)
Br(3)-Bi(1)-Br(5)	95.3 (1)	Br(2)-Bi(2)-Br(3′)	85.7 (1)
Br(4)-Bi(1)-Br(5)	94.1 (1)	Br(6)-Bi(2)-Br(3′)	87.6 (1)
Br(1)-Bi(1)-Br(1′)	87.5 (1)	Br(7)-Bi(2)-Br(3′)	100.1 (1)
Br(2)-Bi(1)-Br(1′)	90.2 (1)	Br(8)-Bi(2)-Br(3′)	165.8 (1)
Br(3)-Bi(1)-Br(1′)	87.7 (1)	Bi(1)-Br(1)-Bi(2)	95.6 (1)
Br(4)-Bi(1)-Br(1′)	175.7 (1)	Bi(1)-Br(1)-Bi(1′)	92.5 (1)
Br(5)-Bi(1)-Br(1′)	82.9 (1)	Bi(2)-Br(1)-Bi(1′)	91.1 (1)
Br(1)-Bi(2)-Br(2)	78.7 (1)	Bi(1)-Br(2)-Bi(2)	101.4 (1)
Br(1)-Bi(2)-Br(6)	102.2 (1)	Bi(1)-Br(3)-Bi(2′)	96.5 (1)
Br(2)-Bi(2)-Br(6)	173.2 (1)		

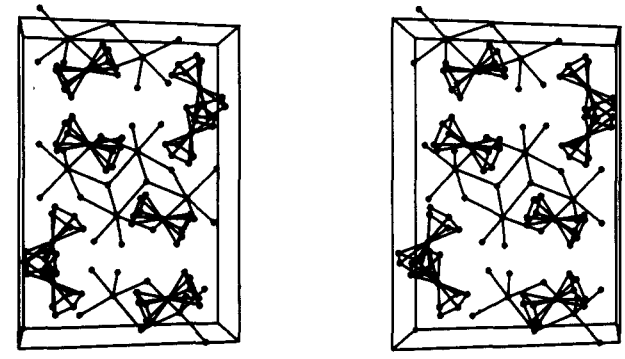

Figure 1. Stereoview of the unit cell for $[(\eta^5\text{-}C_5H_5)_2Fe]_4[Bi_4Br_{16}]$ as viewed along the c crystallographic axis.

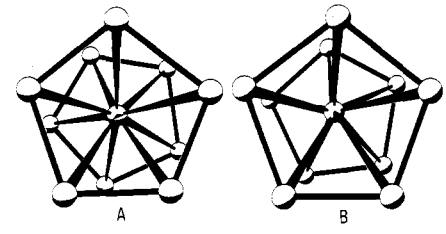

Figure 2. Inter-ring rotational alignment for the two independent ferrocenium ions in $[(\eta^5\text{-}C_5H_5)_2Fe]_4[Bi_4Br_{16}]$: A, environment of Fe(1), 23.4° alignment; B, environment of Fe(2), 7.8° alignment. A symmetrically staggered alignment would require a 36° displacement.

(13) Petterson, R. C. Ph.D. Thesis, University of California, Berkeley, CA, 1966; *Diss. Abstr. B* **1966**, *27*, 3894.
(14) Schleuter, A. W.; Gray, H. B. "Program and Abstracts", Summer Meeting of the American Crystallographic Association, Iowa State University, Ames, IA, Aug 15–20, 1971; American Crystallography Association: 1971; paper D9, p 41.

Table IV. Representative Examples of Polybromobismuthate Anions

no.	compd	struct of polybromobismuthate ion	av Bi-Br bond dist, Å	bond type[a]	ref
I	$[(CH_3)_2NH_2]_3BiBr_6$	octahedron (structure contains two independent anions)	2.845	T, T	20
II	$[(C_6H_5)_4P]_3[Bi_2Br_9]$	two face-sharing octahedra	2.749	T, μ	21
III	$K_4[Bi_2Br_{10}]\cdot 4H_2O$	two edge-sharing octahedra	2.765	T, μ	22
			2.844	T, T	
			2.993	μ	
IV	[picolinium]$BiBr_4$	infinite chain of $BiBr^{3-}$ edge-sharing octahedra	2.64	T, μ	12
			3.04		
V	[piperidinium]$_2BiBr_5$	infinite chain of $BiBr_6^{3-}$ apex-sharing octahedra	2.672	T, μ	23
			2.857		
			3.072		
VI	$[(\eta^5\text{-}C_5H_5)_2Fe]_4[Bi_4Br_{16}]$	cluster of four edge-sharing octahedra	2.683	T, μ	this work
			3.052	μ	

[a] T = terminal, μ = bridging; second symbol refers to the type of bond trans to it.

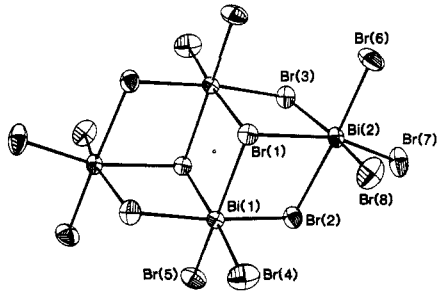

Figure 3. Structure and labeling scheme for the $Bi_4Br_{16}^{4-}$ anion. The anion possesses an inversion center.

eclipsed, as is evident in the views provided in Figure 2. In one case (Fe(1)) the rotational displacement from an eclipsed configuration is 23.4° and in the other (Fe(2)) is 7.8°.[17] We have been unable to locate other examples of unsubstituted metallocenes or their molecular redox products with ring–ring configurations other than staggered or eclipsed.[18] Electron density contour maps of the space containing the rings fail to reveal any indication that the unusual ring displacement is the product of an unreconciled disorder in the carbon atoms. Given that ferrocene (in the gas phase at 140 °C) has a barrier to rotation of only 0.9 ± 0.3 kcal/mol,[19] it is curious that more examples of intermediate rotational configurations are not known. In the present structure, it is possible that a minor decrease in interionic distances produced by unusual rotational realignments could lead to improvements in lattice energy.

The Hexadecabromotetrabismuthate Ion. The structurally novel $Bi_4Br_{16}^{4-}$ ion is derived from four $BiBr_6$ edge-sharing octahedra situated about a crystallographic center of symmetry. The anion-labeling scheme is shown in Figure 3. The shared edges are those formed by the nonbonding vectors between the bridging bromine atoms, Br(1), Br(2), and Br(3). The coordination geometries about Bi(1) and Bi(2) show considerable distortion from idealized octahedra as is evident from an inspection of the bond angles in Table II. The coordination sphere for Bi(1) consists of four bridging and two terminal bromine atoms, whereas the environment of Bi(2) consists of three bridging and three terminal bromine atoms. Br(1) bridges three bismuth atoms (the first example among polyhalobismuthates), while Br(2) and Br(3) each bridge two bismuth atoms. As would be expected, the terminal Bi–Br bonds (average 2.683 (4) Å) are considerably shorter than the bridging Bi–Br bonds (average 3.052 (4) Å). Bi–Br bonds to the triply bridging bromine atom, Br(1) (average 3.13 Å), are longer than those to the doubly bridging bromine atoms, Br(2) and Br(3) (average 3.00 Å), but the ranges overlap: triple-bridge range, 3.10–3.16 Å; double-bridge range, 2.84–3.14 Å.

Table IV provides representative examples of all crystallographically characterized types of polybromobismuthate ions. All anion structures are based upon single or associated distorted octahedra. All three possible modes of association, face, edge, and apex sharing, are found: $Bi_2Br_9^{3-}$, two face-sharing octahedra;[21] $Bi_2Br_{10}^{4-}$, two edge-sharing octahedra;[20,22] $(BiBr_4^-)_\infty$, infinite-chain, edge-sharing octahedra;[12] $Bi_4Br_{16}^{4-}$, cluster of four edge-sharing octahedra; and $BiBr_5^{2-}$, infinite chain of apex-sharing octahedra.[23] The Bi–Br bond distances in these octahedra fall clearly into three groups: terminal, trans to a μ-Br (average 2.70 Å); terminal, trans to a terminal Br (average 2.85 Å); and bridging (average 3.05 Å). The same trans effect has also been observed in vibrational studies of many of these compounds through an analysis of force constants.[24] Huheey[25] has observed that when the Bi^{3+} ion is forced into a high-symmetry environment, the ion assumes a spherical shape but that, in lower symmetry environments, the $6s^2$ lone pair is stereochemically active and leads to distortions of octahedral symmetry as seen in the polybromobismuthates. Since similar distortions are also seen in $BiBr_6^{3-}$ ions in which all Bi–Br bonds are terminal,[20,26] the distortions in the present case are all not likely the sole result of the combination of bridging and terminal bonds.

Acknowledgment. This work was, in part, supported by the National Science Foundation, which also provided funds for the purchase of the X-ray diffractometer.

Registry No. $[(\eta^5\text{-}C_5H_5)_2Fe]_4[Bi_4Br_{16}]$, 87136-13-8.

Supplementary Material Available: Tables 1S–5S listing bond distances, bond angles, anisotropic thermal parameters, calculated hydrogen atom coordinates, and observed and calculated structure factors, respectively (24 pages). Ordering information is given on any current masthead page.

(15) Bernstein, T.; Herbstein, R. H. *Acta Crystallogr., Sect. B* **1968**, *B24*, 1640.
(16) Bats, J. W.; de Boer, J. S.; Bright, D. *Inorg. Chim. Acta* **1971**, *5*, 605.
(17) The angles in question were calculated as the average of the dihedral angles defined as (ring carbon atom)–(centroid)–(centroid)–(ring carbon atom).
(18) Churchill, M. R.; Wormald, J. *Inorg. Chem.* **1969**, *8*, 716.
(19) Haaland, A.; Nilsson, J.-E. *Chem. Commun.* **1968**, 88. Bohn, R. K.; Haaland, A. *J. Organomet. Chem.* **1966**, *5*, 470.
(20) McPherson, W. G.; Myers, E. A. *J. Phys. Chem.* **1968**, *72*, 3117. The same structure is also found in $Na_7[BiBr_6][Bi_2Br_{10}]\cdot 18H_2O$: Lazarine, F. *Acta Crystallogr., Sect. B* **1980**, *B36*, 2748.
(21) Lazarini, F. *Acta Crystallogr., Sect. B* **1977**, *B33*, 2686.
(22) Lazarini, F. *Acta Crystallogr. Sect. B* **1977**, *B33*, 1954.
(23) McPherson, W. F.; Meyers, E. A. *J. Phys. Chem.* **1968**, *72*, 532.
(24) Laane, J.; Jagodzinski, P. W. *Inorg. Chem.* **1980**, *19*, 44.
(25) Huheey, J. "Inorganic Chemistry", 2nd ed.; Harper and Row: New York, 1978; p 208 and references contained therein.
(26) Lazarini, F. *Acta Crystallogr., Sect. B* **1978**, *B34*, 2288.